



ارائه شده توسط:

سایت ترجمه فا

مرجع جدیدترین مقالات ترجمه شده

از نشریات معتبر

# Robust PSS Parameters Design Using a Trajectory Sensitivity Approach

S. Q. Yuan and D. Z. Fang

**Abstract**—A new model for coordinated optimal design of power system stabilizers (PSSs) is proposed for damping low frequency power oscillation of interconnected power systems and enhancing overall performance of both transient and small-signal stability. In this model, a novel objective function is constructed using rotor speeds of generators in a post disturbed period. Trajectory sensitivity mapping technique is proposed to evaluate the approximate gradients of the objective function relative to the PSS parameters. With the gradients, conjugate gradient method is employed to assess the PSS parameters for minimizing the objective function. Two schemes of gradient formulation and optimization procedure are suggested and compared. The model and effectiveness of the method are verified by eigenvalue assessments and time domain nonlinear simulations on the IEEE four-generator and the ten-generator New England test systems.

**Index Terms**—Optimization methods, power system dynamic stability, sensitivity analysis.

## I. INTRODUCTION

IN modern interconnected power systems, power system stabilizer (PSS) is widely utilized to damp low frequency power oscillations and to improve small signal stability [1]. Generally, a PSS design includes two aspects, the choice of the PSS installation site and the design of the PSS parameters. Eigenvalue analysis and participation methods [1], [2] have been used in the problem of selection PSS site. Various methods such as electric torque analysis, phase compensation and pole replacement [3]–[6] have been proposed and utilized in the design of PSS parameters. New methods in robust design of PSS parameter have been appeared in more recent literatures [7]–[11]. However, all these PSS parameter design methods are based on a linear system model of power systems at a certain operating point.

One shortcoming for an effective PSS setting for small-signal stability is that the synchronizing torque may be impaired following a large disturbance [2]. A viable way to overcome this is a discontinuous excitation control scheme called transient stability excitation control [1], whose implementation sometimes needs remote telemetered signals. This paper proposes a trajectory sensitivity based method to address this problem, i.e., to

Manuscript received January 17, 2007; revised October 13, 2008. First published February 27, 2009; current version published April 22, 2009. This work was supported by the Natural Science Foundation of China under Grant No. 50777046, in part by the Doctoral Foundation of Ministry of Education of China under Grant No. 06D0006, and in part by the National Basic Research Program of China under Grant No. 2004CB217904. Paper no. TPWRS-00023-2007.

The authors are with the Key Laboratory of Power System Simulation and Control of Ministry of Education of China, Tianjin University, 300072 Tianjin, China (e-mail: esqyuan@yahoo.com.cn).

Digital Object Identifier 10.1109/TPWRS.2008.2012192

enhance both small and large-signal stability by one PSS parameter setting only.

Trajectory sensitivity approach was originally applied in the system control and parameter estimation [12], [13]. A method for trajectory sensitivity simulation of hybrid differential and algebraic discrete systems has been reported in [14]. Recently it has also been successfully applied in analysis of grid disturbance [15], in transient stability analysis and control [12], [16]–[18] and in tuning limiter of system nonlinear controller [19], [20].

Approach of nonlinear trajectory simulation has been widely utilized in verifying the effect of PSS parameter design [7]–[11]. Trajectory sensitivity enables us to extrapolate the system dynamic behavior for a small change in system parameters. It is possible to extend its applications to the area of optimal PSS parameter design for enhancing system overall stability by damping low frequency oscillations. In this paper, an objective function represented by generator speeds is introduced to measure the PSS effect on damping system oscillations. A trajectory sensitivity mapping technique is developed to evaluate the gradient of the objective function with respect to PSS parameters and to coordinately tune PSS parameters. Case studies on the four-generator and the ten-generator New England test systems validate effectiveness of the approach on PSS parameter design.

The organization of this paper is as follows. Section II presents the basic formulation of trajectory sensitivity in power system model. The model and methodology for robust setting of PSS parameters is established in Section III. Sections IV and V are case studies and conclusions.

## II. MODELS FOR TRAJECTORY SENSITIVITY ASSESSMENT

The dynamic model of a multimachine power system can generally be described by the following differential-algebraic equations (DAE).

$$\dot{\mathbf{x}} = \mathbf{f}(\mathbf{x}, \mathbf{y}, \boldsymbol{\alpha}), \quad \mathbf{x}(t_0) = \mathbf{x}_0 \quad (1)$$

$$\mathbf{0} = \mathbf{g}(\mathbf{x}, \mathbf{y}, \boldsymbol{\alpha}), \quad \mathbf{y}(t_0) = \mathbf{y}_0 \quad (2)$$

where vectors  $\mathbf{x}$  and  $\mathbf{y}$  stand for state and algebraic variables; vector  $\boldsymbol{\alpha}$  for PSS parameters to be tuned. Fig. 1 provides the block diagram of a typical lead-lag PSS [1] together with a thyristor-type excitation system, where the input signal for PSS,  $\Delta\omega = \omega - \omega_r$  is the deviation of the generator rotor speed  $\omega$  from the system synchronous speed  $\omega_r$ . Assume that in the PSS parameter design, the time constant of the washout filter,  $T_w$ , the

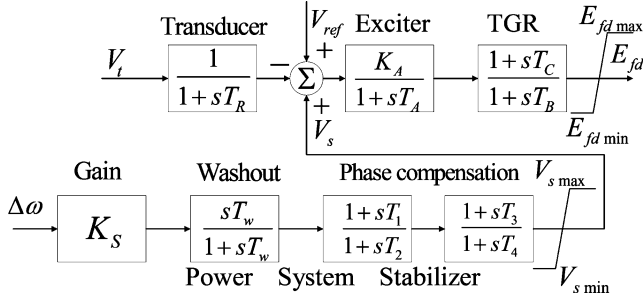


Fig. 1. Structure of thyristor-type excitation system and PSS used in the studies.

lead-lag time constants,  $T_2$  and  $T_4$ , and the bounds of PSS output signal,  $V_{S\max}$  and  $V_{S\min}$  are prespecified parameters, and the gain factor,  $K_S$ , the phase lead-lag time constants,  $T_1$  and  $T_3$ , are the PSS parameters to be designed. The assumption implies that parameter vector  $\alpha$  in (1)–(2) consists of  $K_S$ ,  $T_1$  and  $T_3$  of all considered PSSs. The excitation system is described in the Appendix.

DAE system (1)–(2) represent a trajectory system. Time domain trajectory solutions of (1)–(2),  $\mathbf{x}(t)$  and  $\mathbf{y}(t)$ , can be obtained by a numerical integration algorithm, such as the implicit trapezoidal rule based sub-tree reduction method [21].

For system (1)–(2), the trajectory sensitivity with respect to parameter vector  $\alpha$  can be expressed by the following [12]:

$$\mathbf{x}_\alpha = \frac{\partial \mathbf{x}(t_0)}{\partial \alpha} + \int_{t_0}^t (\mathbf{f}_x(\mathbf{x}, \mathbf{y}, \alpha) \mathbf{x}_\alpha + \mathbf{f}_y(\mathbf{x}, \mathbf{y}, \alpha) \mathbf{y}_\alpha + \mathbf{f}_\alpha(\mathbf{x}, \mathbf{y}, \alpha)) dt \quad (3)$$

where notation definitions are:  $\mathbf{f}_x \triangleq \partial \mathbf{f}(\mathbf{x}, \mathbf{y}, \alpha) / \partial \mathbf{x}$ ,  $\mathbf{f}_y(\mathbf{x}, \mathbf{y}, \alpha) \triangleq \partial \mathbf{f}(\mathbf{x}, \mathbf{y}, \alpha) / \partial \mathbf{y}$ ,  $\mathbf{f}_\alpha(\mathbf{x}, \mathbf{y}, \alpha) \triangleq \partial \mathbf{f}(\mathbf{x}, \mathbf{y}, \alpha) / \partial \alpha$ ,  $\mathbf{x}_\alpha \triangleq \partial \mathbf{x} / \partial \alpha$  and  $\mathbf{y}_\alpha \triangleq \partial \mathbf{y} / \partial \alpha$ , respectively. It is easy to see that  $\partial \mathbf{x}(t_0) / \partial \alpha = 0$  due to  $\mathbf{x}_0$  in (3) is independent on  $\alpha$ . Hence (3) can be represented by the following:

$$\dot{\mathbf{x}}_\alpha = \mathbf{f}_x(\mathbf{x}, \mathbf{y}, \alpha) \mathbf{x}_\alpha + \mathbf{f}_y(\mathbf{x}, \mathbf{y}, \alpha) \mathbf{y}_\alpha + \mathbf{f}_\alpha(\mathbf{x}, \mathbf{y}, \alpha). \quad (4)$$

Similarly in definition of  $\mathbf{g}_x(\mathbf{x}, \mathbf{y}, \alpha) \triangleq \partial \mathbf{g}(\mathbf{x}, \mathbf{y}, \alpha) / \partial \mathbf{x}$ ,  $\mathbf{g}_y(\mathbf{x}, \mathbf{y}, \alpha) \triangleq \partial \mathbf{g}(\mathbf{x}, \mathbf{y}, \alpha) / \partial \mathbf{y}$  and  $\mathbf{g}_\alpha(\mathbf{x}, \mathbf{y}, \alpha) \triangleq \partial \mathbf{g}(\mathbf{x}, \mathbf{y}, \alpha) / \partial \alpha$ , the following can be derived by differentiating both sides of (2) with respect to parameter vector  $\alpha$ :

$$\mathbf{0} = \mathbf{g}_x(\mathbf{x}, \mathbf{y}, \alpha) \mathbf{x}_\alpha + \mathbf{g}_y(\mathbf{x}, \mathbf{y}, \alpha) \mathbf{y}_\alpha + \mathbf{g}_\alpha(\mathbf{x}, \mathbf{y}, \alpha). \quad (5)$$

Equations (4) and (5) describe a linear time-varying system, whose time domain solutions are called  $\alpha$ -trajectory sensitivity in [12].

Let  $\mathbf{x}^k = \mathbf{x}(t_k)$ ,  $\mathbf{y}^k = \mathbf{y}(t_k)$ ,  $\mathbf{x}_\alpha^k = \mathbf{x}_\alpha(t_k)$  and  $\mathbf{y}_\alpha^k = \mathbf{y}_\alpha(t_k)$  for short. Assume  $\mathbf{x}^k$  and  $\mathbf{y}^k$  have just been obtained by the implicit trapezoidal integration approach. Using the implicit trapezoidal rule, the  $\mathbf{x}_\alpha^k$  and  $\mathbf{y}_\alpha^k$  can be evaluated by solving the linear algebraic equation shown in the following:

$$\begin{bmatrix} \frac{h}{2} \mathbf{f}_x(\mathbf{x}^k, \mathbf{y}^k, \alpha) - \mathbf{I} & \frac{h}{2} \mathbf{f}_y(\mathbf{x}^k, \mathbf{y}^k, \alpha) \\ \mathbf{g}_x(\mathbf{x}^k, \mathbf{y}^k, \alpha) & \mathbf{g}_y(\mathbf{x}^k, \mathbf{y}^k, \alpha) \end{bmatrix} \begin{bmatrix} \mathbf{x}_\alpha^k \\ \mathbf{y}_\alpha^k \end{bmatrix} = \begin{bmatrix} \mathbf{C}^{k-1} - \frac{h}{2} \mathbf{f}_\alpha(\mathbf{x}^k, \mathbf{y}^k, \alpha) \\ -\mathbf{g}_\alpha(\mathbf{x}^k, \mathbf{y}^k, \alpha) \end{bmatrix} \quad (6)$$

where

$$\begin{aligned} \mathbf{C}^{k-1} &= -\mathbf{x}_\alpha^{k-1} - \frac{h}{2} (\mathbf{f}_x(\mathbf{x}^{k-1}, \mathbf{y}^{k-1}, \alpha) \mathbf{x}_\alpha^{k-1} \\ &\quad + \mathbf{f}_y(\mathbf{x}^{k-1}, \mathbf{y}^{k-1}, \alpha) \mathbf{y}_\alpha^{k-1} \\ &\quad + \mathbf{f}_\alpha(\mathbf{x}^{k-1}, \mathbf{y}^{k-1}, \alpha)) \end{aligned}$$

and  $h$  is the integration time step.

*Comment:* The coefficient matrix on the left-hand side of (6) is exactly the same as the Jacobian-matrix used in the final Newton iteration at each time step of the implicit trapezoidal integration for computation of  $\mathbf{x}^k$  and  $\mathbf{y}^k$ . Hence, the computation burden for trajectory sensitivities  $\mathbf{x}_\alpha^k$  and  $\mathbf{y}_\alpha^k$  at each discrete time  $t_k$  is approximately the same as an extra Newton iteration added at each time step of numerical integration, which is not heavy at all.

### III. MODEL AND APPROACH FOR PSS PARAMETER DESIGN

#### A. Model of PSS Parameter Design

The purpose of the parameter design is to make the PSSs provide proper damping for power oscillations such that the disturbed system can reach its stable equilibrium point as quickly as possible. In understanding that power system oscillations are caused by generator angle swings, the generator speeds for typical disturbances within a time period is used to construct an objective function in the PSS parameter design. For robustness of the designed PSS controller, several typical operational conditions are considered in the form of the objective function. The following equations present the objective function and the constraints of the PSS parameter design model:

$$\min J = h \sum_{k=1}^R \sum_{i=1}^W \sum_{j=1}^Q \tilde{\omega}_{k,i,j}^2 \quad (7)$$

$$s.t. \left. \begin{aligned} K_{Si}^{\min} &\leq K_{Si} \leq K_{Si}^{\max} \\ T_{1i}^{\min} &\leq T_{1i} \leq T_{1i}^{\max} \\ T_{3i}^{\min} &\leq T_{3i} \leq T_{3i}^{\max} \end{aligned} \right\} (i = 1, 2, \dots, W) \quad (8)$$

where  $R$  stands for the number of operating conditions,  $W$  for the number of PSSs considered in the parameter design,  $Q$  for the number of simulation time steps, and  $\tilde{\omega}_{k,i,j}$  for generator rotor speed of a PSS-equipped generator with respect to the

speed center of inertia (COI) [22]. The objective function evaluated with the post-disturbance generator rotor speeds is an implicit function of the PSS parameters. Generally, the generator rotor speeds are obtained by integration of the system (1)–(2) and they are transformed into COI reference by the following:

$$\tilde{\omega}_{k,i,j} = \omega_{k,i,j} - \omega_{k,j}^{\text{COI}} \quad (9)$$

where  $\omega_{k,j}^{\text{COI}} = (1)/(M_T) \sum_{l=1}^N M_l \omega_{k,l,j}$  stands for the system speed COI at step  $j$  for condition  $k$ ;  $M_T = \sum_{l=1}^N M_l$ ;  $N$  is the number of generators of the system and  $M_l$  is the inertia constant of the  $l$ th generator [22].

From (9), sensitivity of  $\tilde{\omega}_{k,i,j}$  to parameter  $\alpha$  (the specific elements of vector  $\alpha$  in the application are discussed in the next two subsections), denoted by  $\tilde{\omega}_{(\alpha)k,i,j}$  (which is also a vector), can be calculated with the following:

$$\tilde{\omega}_{(\alpha)k,i,j} = \omega_{(\alpha)k,i,j} - \frac{1}{M_T} \sum_{l=1}^N M_l \omega_{(\alpha)k,l,j}. \quad (10)$$

At each discrete time  $t_j$ , the  $\omega_{k,l,j}$  and  $\omega_{(\alpha)k,l,j}$  of all generators are obtained by the trajectory and trajectory sensitivity simulation approaches presented in Section II, and then, the  $\tilde{\omega}_{k,i,j}$  and  $\tilde{\omega}_{(\alpha)k,i,j}$  of all generators with PSS to be tuned are evaluated by (9) and (10). At last, the gradient vector of the control objective to the PSS parameters,  $\partial J/\partial \alpha$ , is evaluated by the following:

$$\frac{\partial J}{\partial \alpha} = 2h \sum_{k=1}^R \sum_{i=1}^W \sum_{j=1}^Q \tilde{\omega}_{k,i,j} \tilde{\omega}_{(\alpha)k,i,j}. \quad (11)$$

*Comment:* As the PSS parameters are not explicitly included in the objective function, this gradient vector is not analytical but a numerical one with a similar role. The usefulness of the gradient information lies in its ability to measure the relative effect of each PSS parameter contributing to the power system dynamics near a small neighborhood of the considered typical operation points.

### B. Procedure of PSS Parameter Design

In this subsection, a procedure designed by the classical conjugate gradient method [23] is used to solve the programming model (7)–(8). To prevent from being tracked into local minimum where the power system configuration is small-signal unstable, the initial PSS parameters for the optimization problem are suggested to be derived by the conventional PSS design methods [1]–[11]. Thus, the proposed method concentrates on improving the transient stability without much impairment to the small-signal stability and thus achieves the enhancement of overall system stability.

The PSS parameters can be arranged into a vector as in the following:

$$\alpha \triangleq [\cdots K_{si} \quad T_{1i} \quad T_{3i} \quad \cdots]^T \quad (i = 1, 2, \dots, W). \quad (12)$$

Then the PSS parameter design procedure is summarized as follows (Scheme I).

- Step 1) Set the iteration counter  $m = 0$ , and assign the initial value of PSS parameters  $\alpha^{(m)}$ . Evaluate the initial gradient  $\mathbf{g}^{(0)} = (\partial J)/(\partial \alpha)|_{\alpha^{(0)}}$  by (11). Set the initial search direction  $\mathbf{s}^{(0)} = -\mathbf{g}^{(0)}$ .
- Step 2) In the direction of  $\mathbf{s}^{(m)}$ , golden section method [23] is adopted to search for an optimal step length parameter  $\gamma^{(m)}$  to make the object function  $J(\alpha^{(m+1)})$  minimum on condition that  $\alpha^{(m+1)} = \alpha^{(m)} + \gamma^{(m)}\mathbf{s}^{(m)}$  and that constraint (8) are all satisfied. If  $|J(\alpha^{(m+1)}) - J(\alpha^{(m)})| < \varepsilon$  ( $\varepsilon = 1e-4$  is a tolerance threshold), go to Step 5. The convergence conditions for the golden section method are a tolerance threshold of  $1e-4$  for the objective function and the maximum iteration number of 10.
- Step 3) Evaluate the gradient  $\mathbf{g}^{(m+1)} = (\partial J)/(\partial \alpha)|_{\alpha^{(m+1)}}$  by (11). Calculate the coefficient  $\beta^{(m+1)} = ((\mathbf{g}^{(m+1)} - \mathbf{g}^{(m)})^T \mathbf{g}^{(m+1)}) / ((\mathbf{g}^{(m)})^T \mathbf{g}^{(m)})$  and the new conjugate gradient vector  $\mathbf{s}^{(m+1)} = -\mathbf{g}^{(m+1)} + \beta^{(m+1)}\mathbf{s}^{(m)}$ .
- Step 4) Set  $m = m + 1$  and go back to Step 2.
- Step 5) End.

*Comment:* In Step 2, the upper and lower bounds constrained by (8) can be easily met in the line search problem along a specified conjugate gradient direction. Firstly, the largest interval available for golden section method is found by checking the following, then evaluation of objective function goes and the remaining subinterval dwindles:

$$\begin{aligned} & \min \eta_j \quad (j = 1, 2, \dots, 3W) \\ & s.t. \quad \begin{cases} \eta_j = \frac{\alpha_j^{\max} - \alpha_j^{(m)}}{s_j^{(m)}}, & \text{if } s_j^{(m)} > 0 \\ \eta_j = \frac{\alpha_j^{\min} - \alpha_j^{(m)}}{s_j^{(m)}}, & \text{if } s_j^{(m)} < 0. \end{cases} \end{aligned} \quad (13)$$

In (13), elements  $\alpha_j^{(m)}$  and  $s_j^{(m)}$  are the  $j$ th component of  $3W$ -dimension vectors  $\alpha^{(m)}$  and  $\mathbf{s}^{(m)}$ , respectively. Thus with the minimum nonnegative  $\eta_j$  calculated by (13), the largest interval for golden section search is set as  $[0, \eta_{\min}]$ .

### C. Variant on the Element Formulation of Gradient Vector and the Optimization Procedure

The methodology in the above subsections already seems adequate for the convergence of the conjugate gradient method to reach a local minimum. However, the authors noticed that in the numerical case studies, the candidate range for one-dimension searching, i.e.,  $[0, \eta_{\min}]$  mentioned above, could be too small to reach an effectively new PSS parameter configuration. This situation happens especially when one of the three parameters of a certain PSS is on its bound and the corresponding gradient element tends to enhance that exceeding in the next iteration. To hasten the iterative process and to avoid such a premature local minimum for the optimization procedure, another scheme (Scheme II) is proposed as follows.

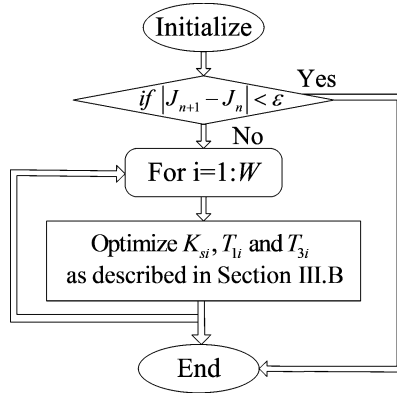


Fig. 2. Iteration procedure for the scheme with a series of lower dimension vectors of PSS parameters.

The previous PSS parameter vector for the entire power system is now decomposed into a series of vectors shown in the following, each belonging to one PSS:

$$\alpha_i \triangleq [K_{si} \quad T_{1i} \quad T_{3i}]^T (i = 1, 2, \dots, W). \quad (14)$$

Then the element formulation for the gradient vector transforms in the same way, e.g.,  $\mathbf{g}_i^{(0)} = (\partial J)/(\partial \alpha_i)|_{\alpha_i^{(0)}}$  is the initial gradient vector for the  $i$ th PSS. Accordingly, PSS parameter design procedure should go sequentially, with one PSS tuned after another. The flowchart is illustrated in Fig. 2. Note that the kernel optimization block is almost unchanged as described in the above subsection except that the notations in the aforementioned steps are appended with subscript  $i$  for each PSS and that in (13)  $3W$  becomes 3. The convergence criterion is that the value of objective function changes little after two successive iterations. The iteration counter  $n$  may be limited to a certain number to stop prolonged iteration if necessary. Fortunately, numerical case studies in the next section converged quickly enough.

#### IV. CASE STUDIES

##### A. Test on the Four-Generator Power System

To show the effect of the PSS on damping the interarea electromechanical mode power oscillation, the proposed method was tested on the four-generator test power system [1] shown in Fig. 3. In the test, all four generators are represented by the double-axis model, and are equipped with PSS and thyristor exciter shown in Fig. 1. The loads are represented by constant impedance. The PSS prespecified parameters, initial values and bounds used in the PSS design method are shown in Table I. Physical implementation is taken into account when the bounds are chosen.

To enhance the robustness of PSS control, three operation conditions are considered in constructing the objective function of (7):

- 1) the base operational condition;
- 2) outage of one of 7–8 lines with loading conditions decreased to 0.95 p.u.;
- 3) 50-MW generation shifts from G3 to G2.

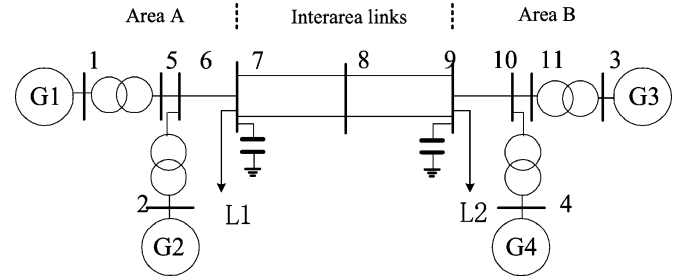


Fig. 3. Configuration of the IEEE four-generator test power system.

TABLE I  
PARAMETERS, INITIAL VALUES, AND BOUNDS FOR  
THE ORIGINAL PSS PARAMETER SETTING

$T_W(s)$	$T_2(s)$	$T_4(s)$	$V_{Smax}(p.u.)$	$V_{Smin}(p.u.)$
10	0.02	5.4	0.2	-0.2
$T_1(s)$	$T_{1max}(s)$	$T_{1min}(s)$	$T_3(s)$	$T_{3max}(s)$
0.05	$4T_1(s)$	$0.1T_1(s)$	3	$4T_3(s)$
$T_{3min}(s)$	$K_S(p.u.)$	$K_{Smax}(p.u.)$	$K_{Smin}(p.u.)$	
$0.1T_3(s)$	20	$4K_S$	$0.1K_S$	

TABLE II  
EIGENVALUES, FREQUENCIES, AND DAMPING RATIOS OF ELECTROMECHANICAL  
MODES FOR THE ORIGINAL PSS PARAMETER SETTING

MACHINE GROUPS	CONDITION 1)	CONDITION 2)	CONDITION 3)
G2 VERSUS G1	$-1.938 \pm j5.738$	$-1.839 \pm j5.628$	$-1.896 \pm j5.817$
G4 VERSUS G3	$-2.165 \pm j5.936$	$-2.096 \pm j5.818$	$-2.128 \pm j5.862$
G3, G4	$0.945\text{HZ}, 0.343$	$0.926\text{HZ}, 0.339$	$0.933\text{HZ}, 0.341$
VERUS G1, G2	$-0.530 \pm j3.504$	$-0.520 \pm j2.845$	$-0.520 \pm j3.406$
	$0.558\text{HZ}, 0.149$	$0.453\text{HZ}, 0.180$	$0.542\text{HZ}, 0.151$

Eigenvalues, their frequencies and damping ratios of electromechanical modes obtained under the three conditions for the original PSS parameter setting are listed in Table II.

The disturbance used in the proposed method is a three-phase short-circuit fault at Bus 8 happened at 0.5 s and cleared at 0.6 s. Such a disturbance could arouse the interarea oscillation in the system. The value of objective function for the base case is 0.2352.

Two schemes of PSS parameter design are conducted, started from the base parameter in Table I. The intermediate conjugate gradient vectors and other information during the iterative process are given in Tables III and IV. Tables V and VI present eigenproperties of electromechanical modes for the resultant PSS parameters. Nonlinear simulations have been performed under the base operation condition for a three-phase short-circuit at Bus 9 cleared after 0.1 s with and without one of 8–9 lines tripped. The swing angles with respect to COI reference are plotted in Figs. 4 and 5.

It can be inferred that both schemes could find a PSS configuration that alleviates the dynamic oscillation post-fault, and the indices for small-signal stability keep meeting common criterion, if not better than the original one. With both the trajectory sensitivity approach and eigenproperty analysis, we can choose a robust PSS parameter design that meets the requirements of both the transient and small-signal stability. Moreover, Scheme

TABLE III  
INTERMEDIATE DATA DURING ITERATIVE PROCESS FOR SCHEME I ON IEEE FOUR-GENERATOR CASE

Iteratio <i>n</i>	$s=[A_1 B_1 C_1 A_2 B_2 C_2 A_3 B_3 C_3 A_4 B_4 C_4]^T$
1	$s=[-4.1\text{e-}6 \ 3.2\text{e-}4 \ -2.5\text{e-}5 \ 2.7\text{e-}6 \ 2.3\text{e-}4 \ 2.4\text{e-}5 \ 4.4\text{e-}6 \ 1.3\text{e-}5 \ 2.5\text{e-}5 \ 1.2\text{e-}5 \ -9.9\text{e-}4 \ 7.3\text{e-}5]^T$ $\alpha=[20 \ 0.0646 \ 2.9989 \ 20 \ 0.0603 \ 3.0011 \ 20 \ 0.0506 \ 3.0012 \ 20 \ 0.005 \ 3.0033]^T$ $\eta_{\min}=45.7, \gamma=45.7, J=0.1859$
2	$s=[-2.6\text{e-}6 \ 2.9\text{e-}4 \ -1.3\text{e-}5 \ 7.1\text{e-}6 \ -7.5\text{e-}5 \ 5.1\text{e-}5 \ 2.6\text{e-}5 \ -2.2\text{e-}4 \ 1.3\text{e-}4 \ 6.5\text{e-}6 \ -5.9\text{e-}4 \ 3.5\text{e-}5]^T$ $\alpha=[20 \ 0.0646 \ 2.9989 \ 20 \ 0.0603 \ 3.0011 \ 20 \ 0.0506 \ 3.0012 \ 20 \ 0.005 \ 3.0033]^T$ $\eta_{\min}=0, \gamma=0, J=0.1856$

\* $A_i, B_i$  and  $C_i$  correlate with  $\partial J/\partial K_{si}$ ,  $\partial J/\partial T_{li}$  and  $\partial J/\partial T_{3i}$ , respectively.

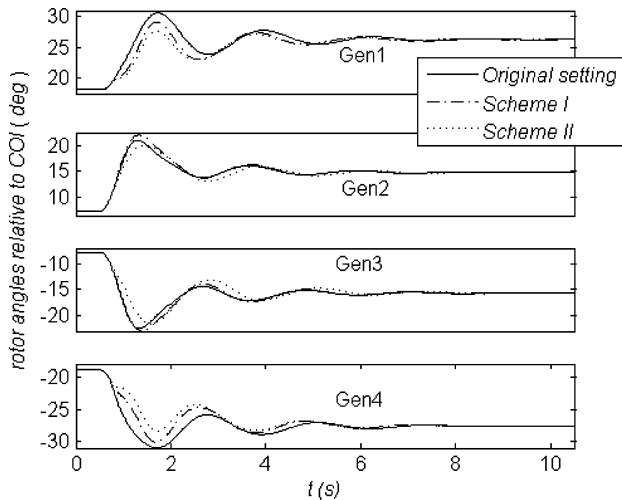


Fig. 4. Swing curves for the contingency with one of Line 8-9 tripped.

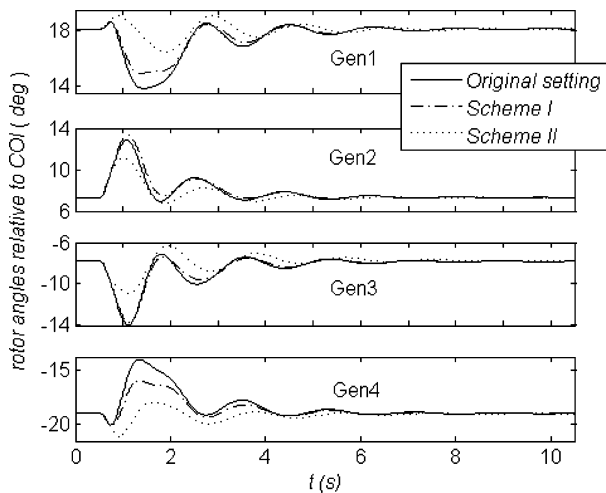


Fig. 5. Swing curves for the contingency without line tripping.

II is better than Scheme I because although both converge after two iterations, Scheme II is better at preventing premature convergence and thus can find a better local optimum.

### B. Test on the New England System

To demonstrate the effectiveness of the proposed method on a larger and more complicated power system, the readily accessible ten-generator 39-bus New England system [24] is adopted.

Fig. 6 shows the configuration of the test system. All generators are represented by the double-axis generator model with both PSS and thyristor-type exciter shown in Fig. 1. To reinforce the nonlinearity during dynamics, all loads are composed of 40% constant impedance component and 60% constant power component.

The PSS prespecified parameters, initial values are shown in Table VII. The bounds for PSS parameters are the same with Table I. To simplify the result presentation, only the base operation condition and Scheme II are considered. In Case 1, a three-phase short-circuit fault at Bus 5 happened at 0.5 s and cleared at 0.6 s is used to cause a large disturbance. The relationship between the value of objective function and the accumulated times of golden search method being applied (described in Step 2 of Scheme I) can be inferred from Fig. 7(a); Fig. 7(b) shows the relationship between the value of objective function and the times of new conjugate gradient direction being calculated. Note that there are ten dots in Fig. 7(b), which means that one iteration in Fig. 2 was conducted. The resultant PSS parameter setting is listed Table VIII, and eigenvalues for electromechanical modes of both PSS parameter settings are plotted in Fig. 8.

The improvement on transient stability can be demonstrated by Figs. 9 and 10, where a three-phase short-circuit fault at Bus 8 happened at 0.5 s and cleared at 0.6 s was simulated. The optimized PSS setting causes smaller amplitudes during transient dynamics. The weakening of damping ratio and real part of eigenvalues in Fig. 8 is compensated by the improvement on transient stability, and thus the overall system stability may be enhanced, if both meet some engineering experience. Nevertheless, a damping ratio less than 0.06 is hardly adequate in this case. So in Case 2, a smaller disturbance, a three-phase short-circuit fault at Bus 5 happened at 0.5 s and cleared 0.05 s later, is used to for the optimization problem instead.

The resultant PSS parameter setting is listed Table IX; the lowering process of objective function along optimization and the resultant eigenvalues for electromechanical modes are plotted in Fig. 11. Fig. 12 is the swing angles simulated with the resultant PSS parameters in Case 2 for the same fault as Figs. 9 and 10.

Note that the two increases in the objective function during iterative process in Fig. 11(a) led to the unaltered PSS parameters for Gen2 and Gen9 in Table IX. This means there are situations

TABLE IV  
INTERMEDIATE DATA DURING ITERATIVE PROCESS FOR SCHEME II ON IEEE FOUR-GENERATOR CASE

Iteratio <i>n</i>	<i>G</i> <sub>1</sub>	<i>G</i> <sub>2</sub>	<i>G</i> <sub>3</sub>	<i>G</i> <sub>4</sub>
1	$A_1=-4.1e-6, B_1=3.2e-4,$ $C_1=-2.5e-5, J=0.1620,$ $\eta_{min}=470.4, \gamma=450.6,$ $\alpha_1=[19.998 \ 0.1937$ $2.9889]$	$A_2=2.7e-6, B_2=2.3e-4,$ $C_2=2.4e-5, J=0.1620,$ $\eta_{min}=662.6, \gamma=0,$ $\alpha_2=[20 \ 0.05 \ 3]$	$A_3=4.4e-6, B_3=1.3e-5,$ $C_3=2.5e-5, J=0.1008,$ $\eta_{min}=11928, \gamma=11928,$ $\alpha_3=[20.053 \ 0.2 \ 3.3036]$	$A_4=1.2e-5, B_4=-9.9e-4,$ $C_4=7.3e-5, J=0.0931,$ $\eta_{min}=45.7, \gamma=45.7,$ $\alpha_4=[20.001 \ 0.005$ $3.0033]$
2	$A_1=6.8e-7, B_1=1.6e-4,$ $C_1=7.7e-6, J=0.0925,$ $\eta_{min}=40.0, \gamma=40.0,$ $\alpha_1=[19.998 \ 0.2 \ 2.9891]$	$A_2=1.7e-6, B_2=5.8e-4,$ $C_2=2.2e-5, J=0.0907,$ $\eta_{min}=257.9, \gamma=46.5,$ $\alpha_2=[20 \ 0.0771 \ 3.001]$	$A_3=1.2e-4, B_3=1.9e-4,$ $C_3=6.9e-4, J=0.0907,$ $\eta_{min}=0, \gamma=0,$ $\alpha_3=[20.053 \ 0.2 \ 3.3036]$	$A_4=3.9e-6, B_4=-1.2e-4,$ $C_4=2.3e-5, J=0.0907,$ $\eta_{min}=0, \gamma=0,$ $\alpha_4=[20.001 \ 0.005$ $3.0033]$

\* $A_i, B_i$  and  $C_i$  are elements of conjugate gradient, and correlate with  $\partial J/\partial K_{si}, \partial J/\partial T_{li}$  and  $\partial J/\partial T_{3i}$ , respectively.

TABLE V  
EIGENVALUES, FREQUENCY, AND DAMPING RATIOS OF ELECTROMECHANICAL MODES FOR THE PSS PARAMETER SETTING DERIVED BY SCHEME I

MACHINE GROUPS	CONDITION 1)	CONDITION 2)	CONDITION 3)
G2 VERSUS G1	$-2.126 \pm j6.309$	$-2.076 \pm j6.157$	$-2.103 \pm j6.224$
G4 VERUS G3	$1.004\text{Hz}, 0.319$	$0.980\text{Hz}, 0.320$	$0.991\text{Hz}, 0.320$
G3, G4 VERUS G1, G2	$-1.952 \pm j5.604$	$-1.850 \pm j5.506$	$-1.901 \pm j5.686$
	$0.892\text{Hz}, 0.329$	$0.876\text{Hz}, 0.318$	$0.905\text{Hz}, 0.318$
	$-0.534 \pm j3.529$	$-0.529 \pm j2.874$	$-0.525 \pm j3.432$
	$0.562\text{Hz}, 0.149$	$0.457\text{Hz}, 0.181$	$0.546\text{Hz}, 0.151$

TABLE VI  
EIGENVALUES, FREQUENCY, AND DAMPING RATIOS OF ELECTROMECHANICAL MODES FOR THE PSS PARAMETER SETTING DERIVED BY SCHEME II

MACHINE GROUPS	CONDITION 1)	CONDITION 2)	CONDITION 3)
G2 VERSUS G1	$-2.359 \pm j5.537$	$-2.293 \pm j5.392$	$-2.305 \pm j5.495$
G4 VERUS G3	$0.881\text{Hz}, 0.392$	$0.858\text{Hz}, 0.391$	$0.875\text{Hz}, 0.387$
G3, G4 VERUS G1, G2	$-1.934 \pm j4.965$	$-1.832 \pm j4.913$	$-1.913 \pm j5.051$
	$0.790\text{Hz}, 0.363$	$0.792\text{Hz}, 0.349$	$0.804\text{Hz}, 0.354$
	$-0.521 \pm j3.333$	$-0.501 \pm j2.739$	$-0.514 \pm j3.246$
	$0.530\text{Hz}, 0.154$	$0.436\text{Hz}, 0.180$	$0.517\text{Hz}, 0.156$

where no acceptable step is found along the given conjugate gradient direction. By comparison of Cases 1 and 2, it can be seen that the already good transient dynamics worsen little while adequate small-signal stability could be retained through changing the dynamic conditions used in optimization process.

Another verifiable way for checking improved transient stability by the proposed method is to check the critical clearing time (CCT) for a three-phase short-circuit fault at Bus 14 cleared by tripping Line 14–15. The CCTs for the base case, Cases 1 and 2 are 0.04 s, 0.20 s and 0.23 s, respectively, from which it can be concluded that the transient stability is greatly enhanced without too much deterioration in small-signal stability.

V. CONCLUSION

A trajectory sensitivity-based robust PSS parameters design method is developed in this paper. A new control objective func-

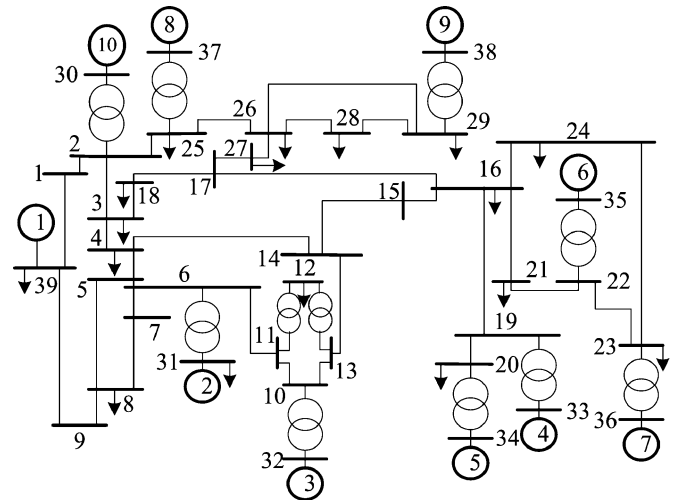


Fig. 6. Configuration of the ten-generator 39-bus New England test power system.

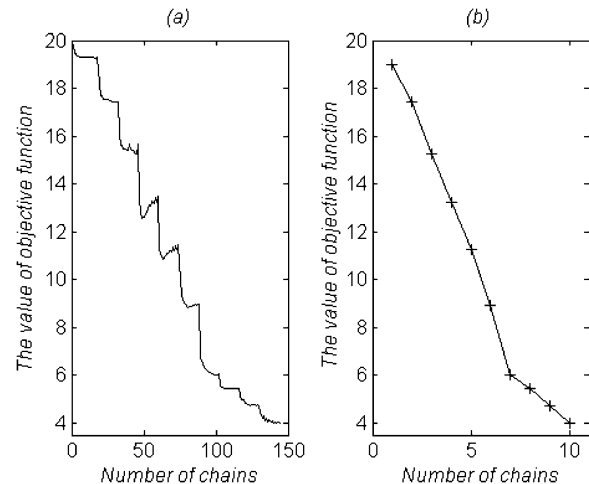


Fig. 7. Relationships between the value of objective function and the number of (a) PSS parameters and (b) new conjugate gradient being evaluated for Case 1, respectively.

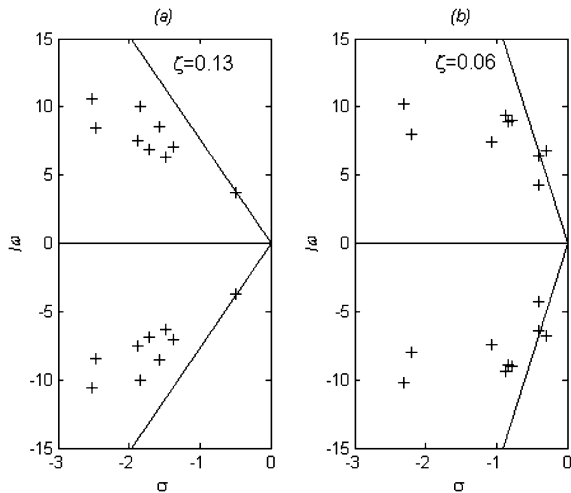


Fig. 8. Eigenvalues for electromechanical modes (a) before and (b) after optimization for Case 1, respectively.

TABLE VII  
PARAMETERS, INITIAL VALUES, AND BOUNDS FOR THE ORIGINAL PSS PARAMETER SETTING

	$K_S(p.u.)$	$T_W(s)$	$T_1(s)$	$T_2(s)$	$T_3(s)$	$T_4(s)$
GEN1	1.0	10	5.0	0.60	3.0	0.50
GEN2	0.5	10	5.0	0.40	1.0	0.10
GEN3	0.5	10	3.0	0.20	2.0	0.20
GEN4	2.0	10	1.0	0.10	1.0	0.30
GEN5	1.0	10	1.5	0.20	1.0	0.10
GEN6	4.0	10	0.5	0.10	0.5	0.05
GEN7	7.5	10	0.2	0.02	0.5	0.10
GEN8	2.0	10	1.0	0.20	1.0	0.10
GEN9	2.0	10	1.0	0.50	2.0	0.10
GEN10	1.0	10	1.0	0.05	3.0	0.50

TABLE VIII  
PARAMETERS DERIVED BY SCHEME II FOR CASE 1

	$K_S$	$T_1$	$T_3$		$K_S$	$T_1$	$T_3$
GEN10	1	1	3	GEN2	1	5	1.001
GEN3	0.928	3	2	GEN4	1.881	0.655	0.655
GEN5	0.726	1.284	0.655	GEN6	2.567	0.158	0.220
GEN7	7.382	0.036	0.479	GEN8	1.718	0.311	0.311
GEN9	2.987	0.150	2.234	GEN1	2	5.207	3.349

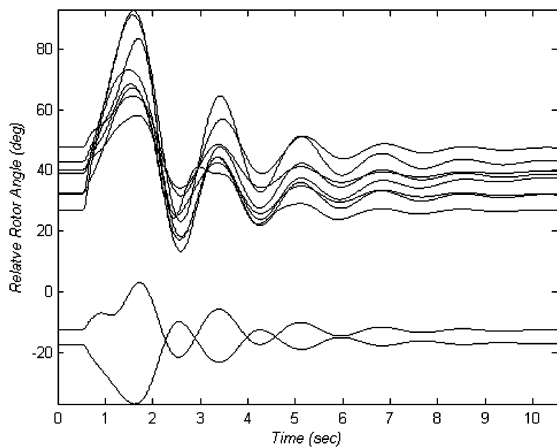


Fig. 9. Swing curves relative to COI for the base PSS setting.

tion represented by rotor speeds of PSS-installed generators in post-disturbance period is utilized. The aim is to improve transient stability while retaining small-signal stability and thus to

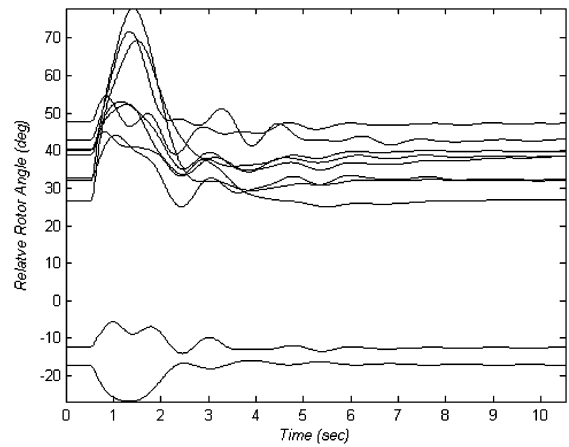


Fig. 10. Swing curves relative to COI for Case 1.

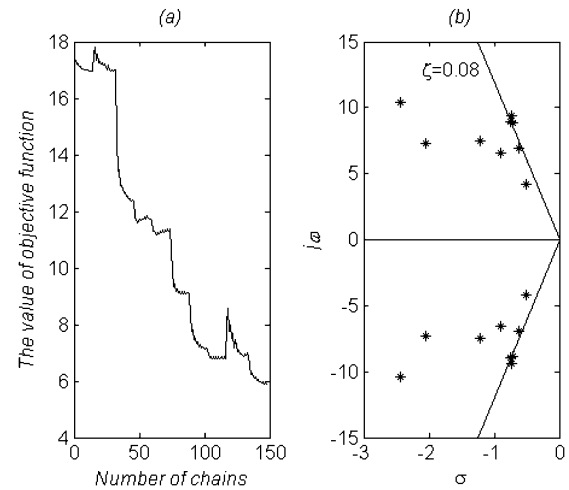


Fig. 11. For Case 2: (a) relationships between the value of objective function and the number of PSS parameters being evaluated; (b) eigenvalues for electromechanical modes after optimization.

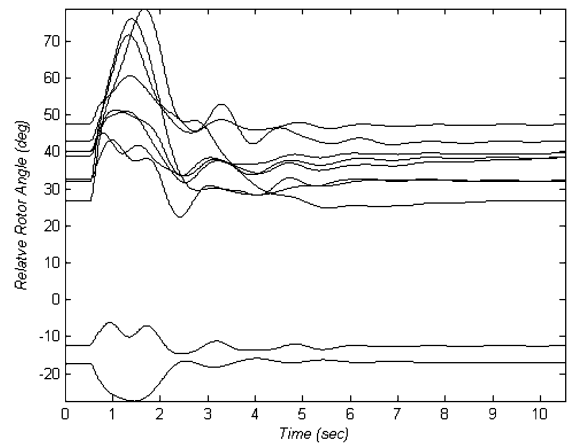


Fig. 12. Swing curves relative to COI for Case 2.

enhance overall system stability. Gradient of the objective function is evaluated through trajectory sensitivity mapping techniques. Using the gradients, the optimization problem is solved by the conjugate gradient method. The case studies validate that

TABLE IX  
PARAMETERS DERIVED BY SCHEME II FOR CASE 2

	$K_S$	$T_I$	$T_3$		$K_S$	$T_I$	$T_3$
GEN10	2	0.240	3.116	GEN2	0.5	5	1
GEN3	1	2.998	1.997	GEN4	2.199	0.574	0.574
GEN5	0.820	1.304	0.655	GEN6	3.001	0.05	0.099
GEN7	7.370	0.02	0.475	GEN8	1.828	0.1	0.1
GEN9	2	1	2	GEN1	2	5.206	3.346

TABLE X  
PARAMETERS FOR EXCITATION SYSTEM

$T_R$ (s)	$K_A$ (p.u.)	$T_A$ (s)	$T_B$ (s)	$T_C$ (s)	$E_{fdmax}$ (p.u.)	$E_{fdmin}$ (p.u.)
0.01	200	0.015	1	10	5	-5

the PSS parameters designed by the proposed method can effectively damp large power oscillations but still maintain good small-signal stability. This method is of potential for coordinating parameters setting of PSSs and FACTS supplementary stabilizers.

#### APPENDIX

The thyristor-type excitation system shown in Fig. 1 is used throughout this paper, with the parameters listed in Table X [24]. The block TGR stands for transient gain reduction [1].

#### REFERENCES

- [1] P. Kundur, *Power System Stability and Control*. New York: McGraw-Hill, 1994.
- [2] E. V. Larsen and D. A. Swann, "Applying power system stabilizers," *IEEE Trans. Power App. Syst.*, vol. PAS-101, pt. I-III, pp. 3017-3046, Jun. 1981.
- [3] Y. Yu, *Electric Power System Dynamics*. New York: Academic, 1983.
- [4] F. P. Demello, P. J. Nolan, T. F. Laskowski, and J. M. Undrill, "Coordinated application of stabilizers in multimachine power systems," *IEEE Trans. Power App. Syst.*, vol. PAS-99, no. 3, pp. 892-899, May 1980.
- [5] C. T. Tse and S. K. Tse, "Refinement of conventional PSS design in multimachine system by modal analysis," *IEEE Trans. Power Syst.*, vol. 8, no. 2, pp. 598-605, May 1993.
- [6] X. Yang and A. Feliachi, "Stabilization of inter-area oscillation modes through excitation systems," *IEEE Trans. Power Syst.*, vol. 9, no. 1, pp. 494-502, Feb. 1994.
- [7] A. L. B. Do Bomfim, G. N. Taranto, and D. M. Falcao, "Simultaneous tuning of power system damping controllers using genetic algorithms," *IEEE Trans. Power Syst.*, vol. 15, no. 1, pp. 163-169, Feb. 2000.
- [8] M. A. Abido and Y. L. Abdel-Magid, "Optimal design of power system stabilizers using evolutionary programming," *IEEE Trans. Energy Convers.*, vol. 17, no. 4, pp. 429-436, Dec. 2002.
- [9] M. A. Abido, "Optimal design of power system stabilizers using particle swarm optimization," *IEEE Trans. Energy Convers.*, vol. 17, no. 3, pp. 406-413, Sep. 2002.
- [10] Y. L. Abdel-Magid and M. A. Abido, "Optimal multiobjective design of robust power system stabilizers using genetic algorithms," *IEEE Trans. Power Syst.*, vol. 18, no. 3, pp. 1125-1132, Aug. 2003.
- [11] D. Z. Fang, S. Q. Yuan, Y. J. Wang, and T. S. Chung, "Coordinated parameter design of STATCOM stabilizer and PSS using MSSA algorithm," *IET Gen., Transm., Distrib.*, vol. 1, no. 4, pp. 670-678, 2007.
- [12] M. J. Laufenberg and M. A. Pai, "A new approach to dynamic security assessment using trajectory sensitivities," *IEEE Trans. Power Syst.*, vol. 13, no. 3, pp. 953-958, Aug. 1998.
- [13] P. M. Frank, *Introduction to System Sensitivity Theory*. New York: Academic, 1978.
- [14] I. A. Hiskens and M. A. Pai, "Trajectory sensitivity analysis of hybrid systems," *IEEE Trans. Circuits Syst. I*, vol. 47, no. 2, pp. 204-220, Feb. 2000.
- [15] I. A. Hiskens and M. Akke, "Analysis of the Nordel power grid disturbance of January 1, 1997 using trajectory sensitivities," *IEEE Trans. Power Syst.*, vol. 14, no. 3, pp. 987-993, Aug. 1999.
- [16] T. B. Nguyen and M. A. Pai, "Dynamic security-constrained rescheduling of power system using trajectory sensitivities," *IEEE Trans. Power Syst.*, vol. 18, no. 2, pp. 848-854, May 2003.
- [17] K. N. Shubhanga and A. M. Kulkarni, "Determination of effectiveness of transient stability controls using reduced number of trajectory sensitivity computations," *IEEE Trans. Power Syst.*, vol. 19, no. 1, pp. 473-482, Feb. 2004.
- [18] D. Chatterjee and A. Ghosh, "Transient stability assessment of power systems containing series and shunt compensators," *IEEE Trans. Power Syst.*, vol. 22, no. 3, pp. 1210-1220, Aug. 2007.
- [19] I. A. Hiskens, "Systematic tuning of nonlinear power system controllers," in *Proc. 2002 Int. Conf. Control Applications*, Sep. 2002, vol. 1, pp. 19-24.
- [20] J.-W. Park and I. A. Hiskens, "Damping improvement through tuning controller limits of a series FACTS device," in *Proc. IEEE Int. Symp. Circuits and Systems*, May 2005, vol. 5, pp. 5298-5301.
- [21] D. Z. Fang and X. D. Yang, "A new method for fast dynamic simulation of power systems," *IEEE Trans. Power Syst.*, vol. 21, no. 2, pp. 619-628, May 2006.
- [22] A. A. Fouad and S. E. Stanton, "Transient stability of a multi-machine power system part I investigation of system trajectory," *IEEE Trans. Power App. Syst.*, vol. PAS-100, no. 7, pp. 3408-3424, Jul. 1981.
- [23] M. T. Heath, *Scientific Computing: An Introductory Survey*, 2nd ed. New York: McGraw-Hill, 2002.
- [24] [Online]. Available: [http://psdyn.ece.wisc.edu/IEEE\\_benchmarks/index.htm](http://psdyn.ece.wisc.edu/IEEE_benchmarks/index.htm).

**S. Q. Yuan** received the B.Eng. degree from South China University of Technology, Guangzhou, China, in 2003, and the M.Eng. degree from Tianjin University, Tianjin, China, in 2006. He is currently pursuing the Ph.D. degree at Tianjin University.

His research interests are in power system dynamics and control.

**D. Z. Fang** received the Ph.D. degree from The Hong Kong Polytechnic University, Kowloon, in 1995.

He joined the faculty of Tianjin University, Tianjin, China, in 1981 and has been a Professor there since 1999. His research interests are in power system analysis, transient stability, and control.



این مقاله، از سری مقالات ترجمه شده رایگان سایت ترجمه فا میباشد که با فرمت PDF در اختیار شما عزیزان قرار گرفته است. در صورت تمایل میتوانید با کلیک بر روی دکمه های زیر از سایر مقالات نیز استفاده نمایید:

لیست مقالات ترجمه شده ✓

لیست مقالات ترجمه شده رایگان ✓

لیست جدیدترین مقالات انگلیسی ISI ✓

سایت ترجمه فا ؛ مرجع جدیدترین مقالات ترجمه شده از نشریات معتبر خارجی